



Theoretical Study on the Formation of 1-neutron and 2-neutron Halo Nuclei via Decay of Elements in Super-Heavy Region

K. Prathapan¹ K.P. Anjali² and R.K. Biju³

^{1,2,3}Department of Physics, Government Brennan College, Thalassery, Kerala-670106, India

³Department of Physics, Pazhassi Raja N.S.S. College, Mattannur, Kerala-670702, India

¹prathapankodilipram@gmail.com

²332anjali@gmail.com

³bijurkn@gmail.com (Corresponding Author)

ARTICLE INFORMATION

Received: June 18, 2020

Revised: August 31, 2020

Accepted: September 08, 2020

Published Online: November 09, 2020

Keywords:

Halo Nuclei, Cluster Radioactivity



DOI: [10.15415/jnp.2020.81003](https://doi.org/10.15415/jnp.2020.81003)

ABSTRACT

The decay characteristics of 1-neutron and 2-neutron halo nuclei from $^{270-316}116$, $^{272-318}118$ and $^{278-320}120$ even-even nuclei is studied within the frame work of the Coulomb and Proximity Potential Model (CPPM). Halo structure in neutron rich nuclei is identified by calculating the neutron separation energies and on the basis of potential energy considerations. A comparison of the decay half-life is made by considering the halo nuclei as spherical cluster and as deformed nuclei with a rms radius. Further, neutron shell closure at neutron numbers 150, 164 and 184 is identified form the plot of $\log_{10} T_{1/2}$ verses the neutron number of parents. The plots of $Q^{1/2}$ verses $\log_{10} T_{1/2}$ and $-\ln P$ verses $\log_{10} T_{1/2}$ for various halo nuclei emitted from the super-heavy elements are found to be linear showing that Geiger-Nuttall law is applicable to the emission of neutron halo also.

1. Introduction

The stability of a nucleus is mainly determined by the binding energy per nucleon. For stable nuclei, the typical value of binding energy per nucleon is in the range of 6-8 MeV. The addition of protons or neutrons takes the nucleus away from the region of stability and becomes unstable and radioactive. The stability of the nucleus ends at the drip lines where the last nucleons are no longer attached to the nucleus by the strong nuclear interaction [1]. This leads to an important observation in many nuclei near the drip line; the last one or two nucleons, either proton or neutron, are found to be very loosely bounded to the core of the nucleus. The separation energies of such nucleons are very low, typically less than 1 MeV. As a result, these weakly bound nucleons are free to occupy a larger volume and the nuclear matter density distribution is found to be extended more in space leads to a nuclear radius which is much larger than that of the normal nucleus. Such nuclei are known as halo nuclei. Halo can be either a neutron halo or a proton halo [2, 3]. Neutron and proton ‘halo’ became an interesting topic for the nuclear physicist since from its discovery by Tanihata et al. in

1985 [4]. The existence of halo was confirmed by Hansen and Jonson in 1987 based on theoretical calculations [5].

The neutron halo was first observed in weakly bound ^{11}Li nucleus and their existence was confirmed in many nuclei such as ^6He , ^9Be , ^{11}Be , ^{14}Be , ^{14}C , ^{19}C etc. The first neutron halo produced in the laboratory was ^6He from a ^9Be target [6]. Other predicted neutron halo nuclei include ^6He , ^8He , ^{11}Be , ^{12}Be , ^{17}B , ^{19}B , ^{17}C , ^{19}C , ^{20}C , ^{22}C , ^{22}N , ^{19}O , ^{23}O , ^{24}F , ^{26}F , ^{27}F , ^{29}Ne , ^{31}Ne etc. [7-13]. The experimental confirmations of many of these halo nuclei are not yet available.

In halo nuclei, almost half of their life time, the unbound nucleon is beyond the range of the core potential. This acts as a hindrance in applying the shell model or the Mean Field (MF) model approaches to describe the properties of halo nuclei. Even the study of the formation of alpha cluster in heavy and super-heavy nuclei involves detailed mathematical calculations. Calculations based on parameter free microscopic model [14], multi-step shell model method [15] etc., could accurately predict the structure and formation probability of alpha cluster from heavy nuclei like ^{212}Po . In 2017, Chang Xu et al. used a

quartering wave function approach for the microscopic calculations of alpha cluster formation from heavy nuclei [16]. The theoretical models used to describe halo nuclei include, Hartree Bogoliubov model with and without Fock term, Relativistic mean field model with Hartree approximation [17], deformed relativistic Hartree Bogoliubov (DRHB) theory [18]. The structural models include, two body systems [19], three body systems such as all bound, Borromean [20], Tango and Samba [21] configurations. The interaction cross section measurements performed by Tanihata et al. in 1985 to study the large density distribution of ^{11}Li proved that, it as an effective tool for studying the halo nuclei [5]. Currently, the interaction and reaction cross-section studies and measurements are widely used to study the structure and properties of halo nuclei. Recently, in 2014, M. Takechi et al. confirmed the existence of the so far heaviest halo in ^{37}Mg through the measurement of reaction cross-section and N. Kobayashi et al. studied the 1n halo configuration of the same [22, 23]. A large number of studies on the interaction and reaction cross-sections involving halo nuclei near the drip line can be found in the literature [24-28]. In 2009, V. Rotival et al. proposed a new method to investigate the neutron halo nuclei where internal wave-function of the N-body system is decomposed in terms of overlap functions. This approach allows a “model-independent analysis of medium-range and asymptotic properties of the internal one-body density” and provides a quantitative estimate of the number of neutrons participating in the formation of halo [29]. Recently in 2016, Angelo Calci et al. studied the ground state parity inversion and the 1n + ^{10}Be halo structure of ^{11}Be using chiral two- and three-nucleon force and found that only certain interactions that produces extremely large E1 transitions between the bound states are capable of reproducing the parity inversion [30]. The s-orbital halo of ^{29}Ne and the s- or p- orbital halo of ^{31}Ne was predicted by M. Takechi et al. from the measurements of interaction cross sections of Neon isotopes [31].

In addition to this, we would like to mention that we have made an attempt to study the decay possibilities of the 1p-halo nuclei ^8B , $^{11,12}\text{N}$, ^{17}F , ^{23}Al , $^{26,27,28}\text{P}$, and 2p-halo nuclei ^9C , $^{17,18}\text{Ne}$, ^{20}Mg , $^{28,29}\text{S}$ from the parents with $Z = 103$ to 114 [32]. We have also studied [33] the structure of various exotic fragments such as ^7Be , $^{10,11}\text{C}$, $^{13,14,15}\text{O}$, ^{19}Ne , $^{20,21}\text{Na}$ and $^{22,23}\text{Mg}$ by computing the separation energy and decay half-lives. In the present work, we made an attempt to study the possibility for the existence of 1n- and 2n- halo nuclei with $Z = 2 - 20$ through the decay of superheavy elements. The details of the theoretical model used in our study is given in section 2. In section 3, the results of our study and the discussions are presents. The major conclusions are given in the section 4.

2. The Coulomb and Proximity Potential Model

For our study we have used the Coulomb and the Proximity Potential Model. This is a well-established model and is extensively used by K.P. Santhosh et al. for the last one decade [34-36]. The model can be used for accurate predictions of alpha decay chains [35, 36] and heavy particle decays from heavy and superheavy elements [35]. The model has been modified for deformed nuclei by considering the quadrupole, octupole and hexadecapole deformations and is used to study the effect of deformation on the half-life of decay [37].

In this model, the interaction potential barrier is taken the sum of Coulomb, proximity and centrifugal potentials for the touching configuration and for the separated fragments. For the overlap region, a simple power law interpolation is used which was proposed by Y.J. Shi and W.J. Swiatecki [38] in 1985. The importance of the proximity potential is that, it reduces the height of the potential barrier and results of calculations obtained through this model is in good agreement with the experimental data.

For a parent nucleus exhibiting exotic decay, the interacting potential barrier can be written as;

$$V = \frac{Z_1 Z_2 e^2}{r} + V_p(z) + \frac{\hbar^2 l(l+1)}{2\mu r^2}; \text{ for } Z > 10 \quad (1)$$

In the above expression, Z_1 and Z_2 are the atomic numbers of the daughter and the emitted cluster, z is the distance between the near surface of the fragments, r is the distance between the fragment centers, which is given as $r = z + C_1 + C_2$. The quantity l is the angular momentum quantum number, μ is the reduced mass and $V_p(z)$ is the proximity potential. The proximity potential is given by Blocki et al [39, 40] as;

$$V_p(z) = 4\pi\gamma b \left[\frac{C_1 C_2}{(C_1 + C_2)} \right] \Phi \left(\frac{z}{b} \right) \quad (2)$$

where, γ is the nuclear surface tension coefficient, b is the width of nuclear surface (diffuseness), C_i are Siissmann central radii and Φ , the universal proximity potential. These equations are applied to spherical nuclei.

The nuclear surface tension coefficient [41] is given by,

$$\gamma = 0.9517 \left[1 - 1.7826 \left(\frac{N-Z}{A} \right)^2 \right] \text{MeV / fm}^2 \quad (3)$$

where, N , Z and A represents the neutron number, proton number and mass number of the nucleus. The universal proximity potential [41] is given by the expression;

$$\Phi(\varepsilon) = -4.41e^{-\varepsilon/0.7176}, \text{ for } \varepsilon \geq 1.9475 \quad (4)$$

and;

$$\begin{aligned} \Phi(\varepsilon) &= -1.7817 + 0.9270\varepsilon + 0.0169\varepsilon^2 \\ &\quad - 0.05148\varepsilon^3, \text{ for } 0 \leq \varepsilon \leq 1.9475 \end{aligned} \quad (5)$$

where $\varepsilon = (z/b)$ with $b \approx 1$. The Siissmann central radii C_i of fragments are related to the sharp radii R_i as;

$$C_i = R_i - \left(\frac{b^2}{R_i} \right) \quad (6)$$

The sharp radii R_i can be calculated by using an empirical formula in terms of the mass numbers A_i as [41];

$$R_i = 1.28A_i^{1/3} - 0.76 + 0.8A_i^{-1/3} \quad (7)$$

The potential for the overlap region of the barrier is given as;

$$V = a_0(L - L_0)^n, \text{ for } z < 0 \quad (8)$$

In this expression, $L = z + 2C_1 + 2C_2$ and $L_0 = 2C$. The constant a_0 and the parameter n are determined by the smooth matching of the two potentials at the touching point.

The barrier penetrability P can be obtained by using one dimensional WKB approximation and is given as;

$$P = \exp \left\{ -\frac{2}{\hbar} \int_a^b \sqrt{2\mu(V - Q)} dz \right\} \quad (9)$$

where a and b are the turning points given by, $V(a) = V(b) = Q$ and Q is the energy released in the decay process.

Also $\mu = mA_1A_2/A$ is the reduced mass with A_1 and A_2 are the mass numbers of the emitted daughter and cluster nuclei respectively. This integral can be evaluated numerically or analytically to get the half life time of decay as;

$$T_{1/2} = \frac{\ln 2}{\lambda} = \frac{\ln 2}{\nu P} \quad (10)$$

where, $\nu = \frac{\omega}{2\pi} = \frac{2E_V}{h}$, the number of assaults on the barrier per second and E_V is the zero-point vibration energy and is given by the empirical formula of Poenaru et al. [42] as;

$$E_V = Q \left\{ 0.056 + 0.039 \exp \left[\frac{(4 - A_2)}{2.5} \right] \right\}, \text{ for } A_2 \geq 4 \quad (11)$$

The zero-point vibration energy E_V vary only slightly with the mass A_2 of the cluster and "this stability of E_V is a useful property for life-time predictions" [42].

3. Results and Discussion

In the present work, we have studied the decay of 1n- and 2n- halo nuclei with $Z = 10$ through cluster radioactivity from the superheavy elements $^{270-316}116$, $^{272-318}118$ and $^{278-320}120$ by using the Coulomb and Proximity Potential Model (CPPM). The proximity potential was first used by Shi and Swiatecki [38] in an empirical manner and has been quite extensively used over a decade by Gupta et al. [43] in the Preformed Cluster Model (PCM). The CPPM was used by K.P. Santhosh et al. and is well established in predicting the barrier penetrability and half-life of decay of light and heavy clusters in heavy and super-heavy region [44-48]. Also, the CPPM is used for predicting the decay characteristics of proton halo nuclei [49] and neutron halo nuclei [50] in heavy and superheavy region. For a halo nucleus, the separation energy of last one or two nucleons is less than 1 MeV. A neutron halo is known as 1n- halo if the 1n- separation energy is lowest and 2n- halo if the 2n- separation energy is the lowest. In terms of mass excess, the 1- and 2- neutron separation energies are defined as [51],

$$\begin{aligned} S(n) &= -\Delta M(A, Z) + \Delta M(A-1, Z) \\ &\quad + \Delta M_n = -Q(\gamma, n) \end{aligned} \quad (12)$$

and

$$\begin{aligned} S(2n) &= -\Delta M(A, Z) + \Delta M(A-2, Z) \\ &\quad + 2\Delta M_n = -Q(\gamma, 2n) \end{aligned} \quad (13)$$

where $S(n)$ and $S(2n)$ are the 1n- and 2n- separation energies respectively. The quantities; ΔM_n , $\Delta M(A, Z)$, $\Delta M(A-1, Z)$ and $\Delta M(A-2, Z)$ are the mass excess of the neutron, the parent nucleus, mass excess of the daughter nucleus produced during one neutron radioactivity and mass excess of the daughter nucleus produced during two neutron radioactivity respectively. Also $Q(\gamma, n)$ and $Q(\gamma, 2n)$ represents the Q values for one neutron and two neutron radioactivity.

In the region $Z < 10$ the 1n- halo nuclei are ^{11}Be , ^{14}B , ^{15}C , ^{17}C , ^{19}C , ^{22}N , ^{23}O , and $^{24,26}\text{F}$. The 2n- halo nuclei with $Z < 10$ are ^6He , ^8He , ^{11}Li , ^{12}Be , ^{14}Be , ^{17}B , ^{19}B , ^{22}C , and $^{27,29}\text{F}$. These 1-n and 2-n halo candidates are directly taken from a recent work of K.P. Santhosh et al. [50]. For nuclei in the range $Z = 10$ to $Z = 20$, we have calculated the $S(n)$ and, $S(2n)$ of various isotopes using the mass excess table of Wang et al. [52]. These are tabulated and given in table 1. On the basis of our calculation of $S(n)$, the possible

1n- halo candidates in the region $Z = 10 - 20$ are ^{29}Ne , ^{31}Ne , ^{36}Na , ^{37}Na , ^{35}Mg , ^{37}Mg , ^{46}P and ^{55}Ca . The isotopes of $Z = 10 - 20$ nuclei showed a lower 2n- separation energy than 1n- separation energy only for ^{34}Ne and can be considered as a candidate for 2n- halo. Even though the 2n- separation energy of ^8He , ^{12}Be , ^{14}Be , ^{17}B , $^{27,29}\text{F}$ [50] and ^{36}Na are greater than 1MeV, they are considered as candidates for 2n- halo nuclei. A. Leistenschneider et al. in 2001, pointed out that such increases in the neutron separation energies may be due to the collective soft dipole excitations [53]. However, this is not verified experimentally.

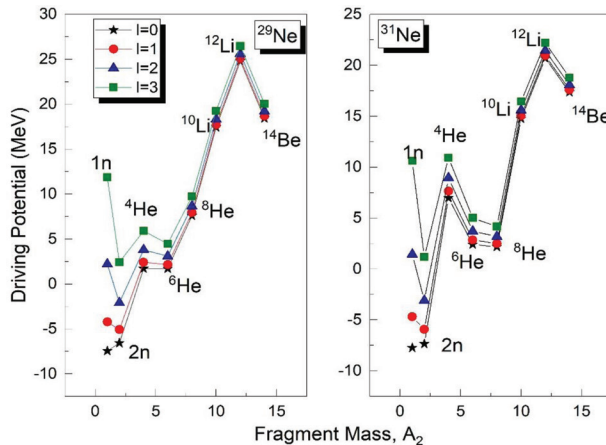


Figure 1: The driving potential ($V - Q$) as a function of the light cluster mass A_2 for n-halo nuclei, ^{29}Ne and ^{31}Ne .

Calculation of neutron separation energy is a basic tool to identify the halo structure in a nucleus. The existence of halo structure in a nucleus can be verified from the calculation of driving potential ($V - Q$) for the touching configuration, where $z = 0$. To calculate the driving potential, we have taken the interaction potential as the sum of Coulomb, proximity and centrifugal potential. The centrifugal part is included by considering $l = 1, 2, 3$ states. The driving potential is calculated for all the halo candidates included in the table 1. A graph is plotted ($V - Q$) verses the fragment mass A_2 , which is the mass of the emitted clusters such as 1n, 2n, ^4He , ^6He , etc. The plots are given the Figures 1, 2, 3, 4 and 5. From the plot of driving potential verses the fragment mass, it is clear that the minimum value of driving potential occurs at $l = 0$ state. The decay probability is maximum when the driving potential is minimum. The importance of the plot is that, we can find a cluster + core configuration with minimum value of the driving potential and a maximum quantum mechanical probability for the existence of halo structure. We have considered different cluster + core configuration for the calculation of driving potential. When we get the deepest minimum for a 1n + core configuration, we consider it as a 1n halo if the 1n

separation energy is less than 1MeV. From Figure 1, it is clear that in the case of $^{29,31}\text{Ne}$, the ($V - Q$) is minimum for the 1n + core configuration. Similarly, Figures 2 to 5; shows that for ^{34}Na , ^{37}Na , ^{37}Mg and ^{55}Ca have also the 1n + core configuration has the deepest minimum corresponding to the most probable configuration. Hence, they can be considered as candidates for 1n- halo nuclei. Similarly, in Figure 2, 3, and 4; we can see that ^{34}Ne , ^{36}Na and ^{40}P shows a 2n + core configuration corresponding to the minimum value of the driving potential. Even though the $S(n)$ of ^{40}P is lower than its $S(2n)$, it can be considered as a 2n- halo since it has a minimum at 2n + core configuration. Therefore, the 2-n halo candidates are ^{34}Ne , ^{36}Na and ^{40}P . From the plot of driving potential, in the case of ^{29}Ne , ^{31}Ne and ^{37}Mg , we can see that with the increase in the angular momentum quantum number (l), the 1n + core configuration is shifted to 2n + core configuration. This kind of changes are observed when the ground state spin and parity of the decays are not conserved [33]. The spin and parity of ^{24}Na , ^{31}Ne and ^{37}Mg are in $\frac{5}{2}^+$, $\frac{3}{2}^+$ and $\frac{5}{2}^-$ respectively and the emission of 1n $\left(\frac{1}{2}^+\right)$ in the $l = 0$ state violates the spin and parity conservation. It has been reported that this kind of observation is possible when the ground state contains a mixture of states with different spin and parities [54] and needs further investigations.

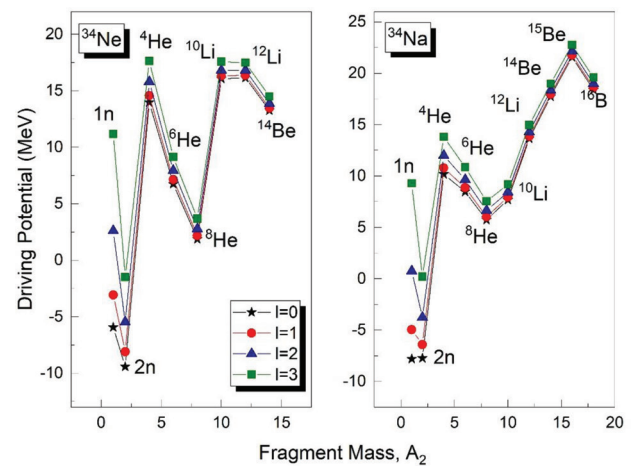


Figure 2: The driving potential ($V - Q$) as a function of the light cluster mass A_2 for n-halo nuclei, ^{34}Na and ^{36}Na .

However, the halo nuclei prefer the lowest angular momentum state ($l = 0$) since large angular momentum will give rise to a centrifugal potential that would tend to confine the nucleons [7]. Only very loosely bound neutrons in an s- state ($l = 0$) relative to the core form an ideal halo; any other angular momentum will ultimately be confined. Only

the s-wave neutrons will show considerable probability of staying outside the potential well at very low separation energies. This is evident from the fact that almost all reported halo nuclei have an s-wave halo structure. Only a very few nuclei such as ^{31}Ne , ^{34}Na and ^{37}Mg exhibit p-wave halo structure [24, 55, 56]. This is also evident from the fact that the formation of neutron halo in many nuclei such as ^{11}Be , ^{14}Be , ^{22}N , ^{23}O and ^{24}F etc., depends directly on the occupation of outer electrons in the $2S_{1/2}$ state [57]. Therefore, we feel that such shifting will not have much effect on the probability for the formation of the halo structure.

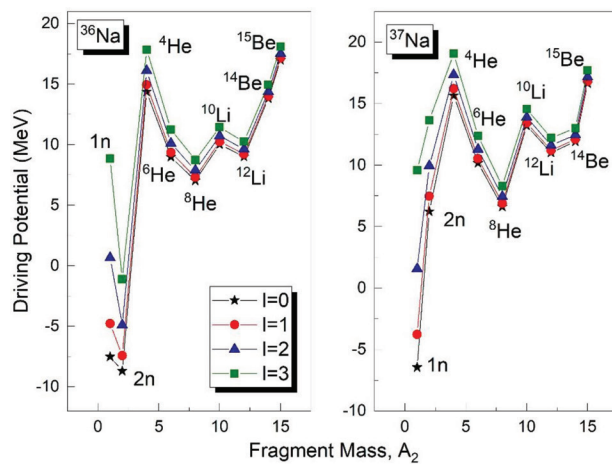


Figure 3: The driving potential ($V-Q$) as a function of the light cluster mass A_2 for n-halo nuclei, ^{36}Na and ^{37}Na .

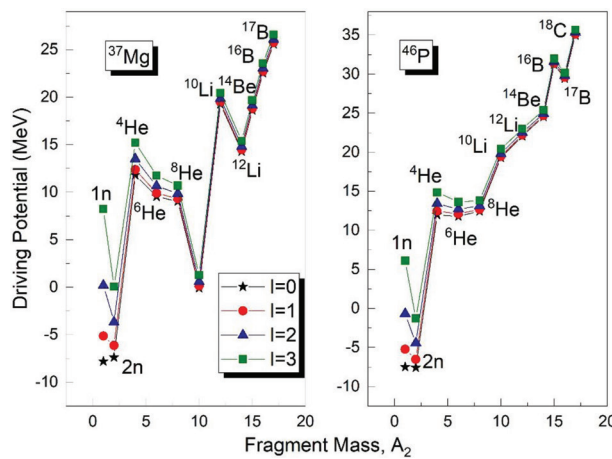


Figure 4: The driving potential ($V-Q$) as a function of the light cluster mass A_2 for n-halo nuclei, ^{37}Mg and ^{46}P .

Further, the angular momentum carried away in the decay of halo nucleus, as appearing in eq. (1) is very small ($\approx 5\hbar$). This small unit of angular momentum will be making considerable contributions to the life time of the emission of light particles, like protons. Its contribution

to half-life of decay of heavy cluster is very small and the angular momentum effects can be neglected [49]. Therefore, in the present study, the calculations are performed assuming zero angular momentum transfers. Also, in this model, the preformation probability is taken as unity for all clusters irrespective of their masses. Cluster radioactivity is energetically possible only when the Q -value of the reaction is greater than zero. The Q -values of the reactions are computed using the tables of KUY [58] using the equation,

$$Q = \left\{ M(A, Z) - M(A_1, Z_1) - M(A_2, Z_2) \right\} + k(Z_{A, Z}^{\varepsilon} - Z_{A_1, Z_1}^{\varepsilon}) \quad (14)$$

where $M(A, Z)$, $M(A_1, Z_1)$ and $M(A_2, Z_2)$ represents the mass excess of the parent, daughter and emitted halo nucleus respectively. The term $k(Z_{A, Z}^{\varepsilon} - Z_{A_1, Z_1}^{\varepsilon})$ is introduced to account for the screening effect of the atomic electrons as suggested by V.Y. Denisov et al. [59]. The value of k and ε depends on the Z value of the parent nucleus. Based on relativistic Hartree-Fock-Slater calculations, K.N. Huang et al. made an estimate of the values of k and ε . For nuclei with $Z \geq 60$, $k = 8.7\text{eV}$ and $\varepsilon = 2.517$. For nuclei with $Z < 60$, they are 13.6 eV and 2.408 respectively [60]. For the emission of 1n-halo nuclei ^{11}Be and ^{14}B the calculated Q -value is very low and value of the decay half-life is very large; far above the experimental limit of 10^{30} seconds. Similarly, for the 2n-nuclei; ^6He , ^8He , ^{11}Li , ^{14}Be , ^{17}B and ^{19}B also the Q -value is very small or even negative and hence are energetically forbidden from majority of the selected superheavy elements except from a very few at the higher mass end; that too with very large values of decay half-life.

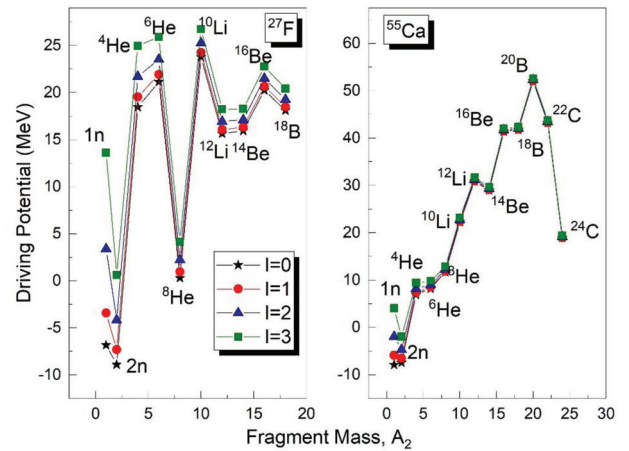


Figure 5: The driving potential ($V-Q$) as a function of the light cluster mass A_2 for n-halo nuclei, ^{27}F and ^{55}Ca .

Table 1: The values of 1n- and 2n- separation energies of halo nuclei and their halo configuration.

Structure	Nucleus	S(n) MeV	S(2n) MeV	Cluster + Core Configuration
1n- halo	^{29}Ne	0.9713	4.7926	1n + ^{28}Ne
	^{31}Ne	0.1713	3.3626	1n + ^{30}Ne
	^{34}Na	0.1713	3.1026	1n + ^{33}Na
	^{37}Na	0.8410	0.8426	1n + ^{36}Na
	^{35}Mg	0.7543	5.4649	1n + ^{34}Mg
	^{37}Mg	0.2413	3.5726	1n + ^{36}Mg
	^{55}Ca	1.2613	5.1026	1n + ^{54}Ca
2n- halo	^{34}Ne	1.2313	0.3026	2n + ^{32}Ne
	^{36}Na	0.0013	1.5226	2n + ^{34}Na
	^{46}P	0.7013	3.6226	2n + ^{44}P

Therefore, in this work we have investigated the possibility for the formation of 1n- halo nuclei ^{15}C , ^{17}C , ^{19}C , ^{22}N , ^{23}O , $^{24,26}\text{F}$, ^{29}Ne , ^{34}Na , ^{37}Na , ^{37}Mg , ^{55}Ca and 2n- halo nuclei, ^{12}Be , ^{27}F , ^{29}F , ^{34}Ne , ^{34}Na , ^{40}P from $^{270-316}116$, $^{272-318}118$ and $^{278-320}120$ through the computation of barrier penetrability and half-life of decay using the CPPM. The half-life for the emission of halo nuclei is calculated by considering them as spherical clusters whose radius is given by the equation (7), where the radius R_i is considered as a function on A_i alone. However, a halo is in a highly deformed nuclear state. The characteristic feature of the halo nucleus is its large root mean square radius. Therefore, we have made a comparison of half-lives of decay by considering the halo nucleus as a spherical cluster with radius R_i and as a deformed nucleus with a rms radius given by [61];

$$\langle R_{rms} \rangle^2 = \langle R_{sph} \rangle^2 \left[1 + \frac{5}{4\pi} \langle \beta_2 \rangle^2 \right] \quad (15)$$

Here, $R_{sph} = R_0 A^{1/3}$ is the radius of the normal nucleus. The quadrupole deformation β_2 is taken from the nuclear data tables of P Moller et al [62]. For the nuclei with $Z < 10$, the rms matter radius is directly taken from the data provided by Suhel Ahmad et al. [63]. For nuclei with $Z = 10$ to $Z = 20$, the rms matter radius is calculated in terms of the quadrupole deformation β_2 using the formula (15), which provides a good approximation to the rms radius of a nucleus including halo. For example, for ^{24}F , the rms radius given in [63] is $3.17 \pm 0.05 \text{ fm}$ and using the equation 15, we get the rms radius of ^{24}F as 3.225 fm .

The results of our calculations are given in the Figures 6-11, where the logarithmic value of decay half-life ($\log_{10} T_{1/2}$) is plotted against the neutron number of parents (N_p). The experimental upper limit of half-life of decay for the detection of a cluster or a halo nucleus is 10^{30} seconds. Based on our calculations, we found that the decay half-life is within or near above the experimental limit only for the emission of ^{15}C , ^{23}O , $^{26,27}\text{F}$, ^{29}Ne and ^{55}Ca halo nuclei. For the emission of other 1n- halo nuclei, ^{17}C , ^{19}C , ^{22}N , ^{26}F , ^{34}Na , ^{37}Na , ^{37}Mg and the 2n- halo nuclei ^{12}Be , ^{29}F , ^{34}Ne , ^{34}Na , ^{40}P , the computed half-life of decay is much larger than the experimental limit. Therefore, it is to be mentioned that the possibility for the emission of 1n- and 2n- halo nuclei from the selected super heavy isotopes is very less. However, we could find certain finite probability for the emission of neutron halo nuclei ^{26}F and ^{55}Ca with a half-life less than 10^{30} seconds and the results are given in Table 2.

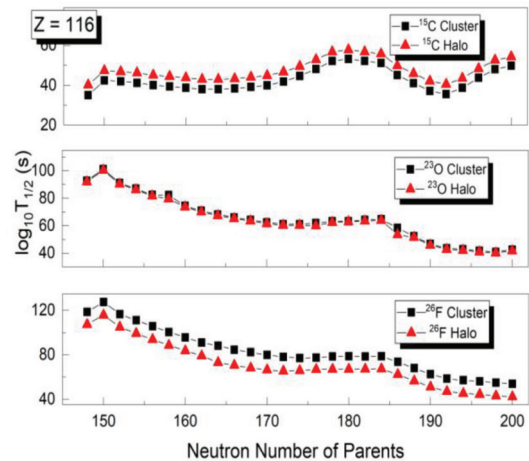


Figure 6: Comparison of the predicted heavy particle decay half-lives of cluster and the neutron halo, ^{15}C , ^{23}O and ^{26}F from $^{264-316}116$ even-even nuclei.

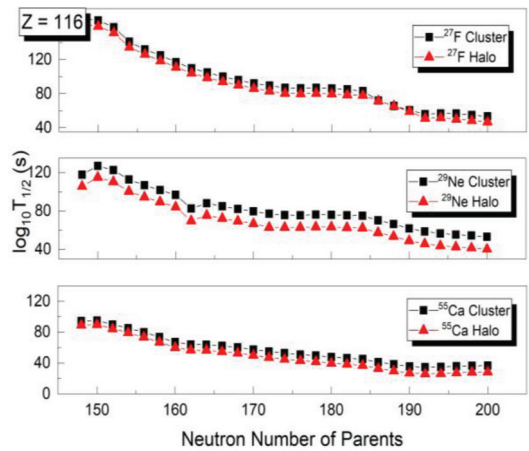


Figure 7: Comparison of the predicted heavy particle decay half-lives of cluster and the neutron halo, ^{27}F , ^{29}Ne and ^{55}Ca from $^{264-316}116$ even-even nuclei.

In Figures 6 and 7, the plot of $\log_{10} T_{1/2}$ verses the neutron number of parents for the emission of various 1n- and 2n-halo nuclei from $^{270-316}116$ even-even nuclei are given. It is observed that, in the case of ^{15}C , the half-life of decay is increased when the normal radius is replaced by rms radius. Similar result was obtained by K.P. Santhosh et al. in the case of decay of ^{15}C nuclei from heavy elements with $Z = 86$ to $Z = 100$ [50]. This is due to the fact that the rms radius (R_{rms}) of ^{15}C is less than the normal radius (R). From the equation

(7), we get the radius as 2.72 fm and the rms radius of ^{15}C is given in reference [63] is 2.59 fm . In the case of other halo nuclei, the rms radius is larger than the normal radius and it is found that the half-life of decay is decreased when the rms radius is included in the calculation. For example, the value of $\log_{10} T_{1/2} = 18.52$ for the decay of ^{26}F from $^{318}118$ when it is considered as a spherical cluster and $\log_{10} T_{1/2} = 16.08$ when ^{26}F is considered as a deformed nucleus with an rms radius.

Table 2: The predicted half-lives for the emission of different neutron halo nuclei from various isotopes of super heavy even-even nuclei by considering the emitted nuclei as cluster and halo nuclei.

Parent Nuclei	Emitted Halo Nuclei	Q-Value (MeV)	Barrier Penetrability P		Decay Constant		$\log_{10} T_{1/2}$ (Sec)	
			Normal	Halo with rms	Normal	Halo with	Normal	Halo with
			Cluster	radius	Cluster	rms radius	Cluster	radius
$^{304}116$	^{55}Ca	159.49	6.15286e-71	1.47167e-62	2.65762e-39	6.35664e-31	38.41	30.03
$^{306}116$	^{55}Ca	160.78	3.37012e-68	9.8528e-60	1.46744e-36	4.29017e-28	35.67	27.20
$^{308}116$	^{55}Ca	161.15	3.73641e-67	1.15953e-58	1.63068e-35	5.06053e-27	34.62	26.13
$^{310}116$	^{55}Ca	160.71	1.3093e-67	3.76612e-59	5.69855e-36	1.63915e-27	35.08	26.62
$^{312}116$	^{55}Ca	160.16	2.77874e-68	7.31583e-60	1.20527e-36	3.17322e-28	35.76	27.33
$^{314}116$	^{55}Ca	159.62	5.94066e-69	1.44108e-60	2.56806e-37	6.22957e-29	36.43	28.34
$^{316}116$	^{55}Ca	159.22	2.23156e-69	5.12496e-61	9.62253e-37	2.20989e-29	36.85	28.49
$^{304}118$	^{26}F	61.28	5.00331e-56	6.16077e-54	8.30433e-34	1.02255e-32	33.80	31.83
$^{306}118$	^{26}F	63.1	8.78037e-52	1.10207e-49	1.50062e-30	1.88351e-28	29.56	27.56
$^{308}118$	^{26}F	65.07	2.28474e-47	2.79834e-45	4.02667e-26	4.93185e-24	25.05	23.16
$^{310}118$	^{26}F	66.44	2.38092e-44	2.74245e-42	4.28453e-23	4.93512e-21	22.18	20.25
$^{312}118$	^{26}F	67.01	2.7185e-43	5.33904e-41	4.93398e-21	9.69017e-20	20.25	18.18
$^{314}118$	^{26}F	67.37	1.99014e-42	3.76787e-40	3.63144e-21	6.87529e-19	20.03	18.13
$^{316}118$	^{26}F	67.93	6.65771e-41	6.54124e-39	1.22494e-19	1.20351e-17	18.76	16.76
$^{318}118$	^{26}F	68.25	3.91806e-40	3.66801e-38	7.24272e-19	6.78053e-17	18.52	16.08
$^{306}118$	^{55}Ca	163.46	4.34311e-61	3.65137e-42	1.92263e-39	1.61641e-30	38.55	29.63
$^{308}118$	^{55}Ca	164.52	9.04595e-59	9.26866e-40	4.03047e-37	4.12975e-28	36.23	27.22
$^{310}118$	^{55}Ca	164.94	1.27735e-57	1.45282e-38	5.70582e-36	6.48964e-27	35.08	26.02
$^{312}118$	^{55}Ca	164.69	1.06117e-57	1.14121e-38	4.73323e-36	5.08997e-27	35.16	26.13
$^{314}118$	^{55}Ca	164.24	3.68357e-58	3.39165e-38	1.63844e-36	1.51319e-26	35.62	25.66
$^{316}118$	^{55}Ca	163.73	9.59738e-59	9.15939e-41	4.25563e-37	4.04902e-29	36.21	28.23
$^{318}118$	^{55}Ca	163.17	2.08798e-58	1.53969e-40	9.25842e-37	6.80389e-29	35.87	28.01
$^{310}120$	^{26}F	67.18	4.3537e-56	4.73995e-49	7.92187e-34	8.32043e-28	33.94	26.92
$^{312}120$	^{26}F	68.68	7.17153e-53	6.8813e-44	1.33405e-31	1.25215e-22	30.71	21.74
$^{314}120$	^{26}F	68.48	3.91537e-53	1.04876e-40	7.26216e-32	1.95091e-19	30.97	18.55
$^{316}120$	^{26}F	69.17	1.32502e-51	5.5987e-41	2.48239e-30	1.03844e-19	29.32	18.82
$^{318}120$	^{26}F	69.77	2.84206e-50	1.77863e-39	5.37071e-29	3.33222e-18	28.11	17.32
$^{320}120$	^{26}F	70.15	2.17089e-49	3.57078e-38	4.12472e-21	6.74777e-17	20.15	16.01
$^{310}120$	^{55}Ca	168.55	2.67283e-59	2.09129e-49	1.25829e-38	9.03754e-28	37.71	26.68

$^{312}_{120}$	^{55}Ca	169.24	9.15381e-60	6.5544e-48	4.29718e-38	2.83284e-26	37.20	25.42
$^{314}_{120}$	^{55}Ca	169.92	2.43016e-59	5.67054e-45	1.14082e-37	2.47863e-26	36.78	25.86
$^{316}_{120}$	^{55}Ca	168.14	2.4152e-58	2.15992e-41	1.13582e-36	9.53708e-25	35.78	24.35
$^{318}_{120}$	^{55}Ca	167.81	1.69562e-57	2.82743e-38	7.98432e-36	1.25924e-25	34.93	24.21
$^{320}_{120}$	^{55}Ca	167.31	5.77315e-57	1.64696e-41	2.71907e-36	5.48443e-26	35.82	25.38

Figures 8 and 9 are the plots of $\log_{10} T_{1/2}$ versus the neutron number of parents for the emission of ^{15}C , ^{23}O , $^{26,27}\text{F}$, ^{29}Ne and ^{55}Ca nuclei from $^{272-318}118$ even-even nuclei. The results are similar to that of the decay from $^{270-316}116$ nuclei. Except for ^{15}C , the half-life of decay is lower for the halo than the spherical cluster. The plot of $\log_{10} T_{1/2}$ versus the neutron number of parents for the emission of various 1n- and 2n- halo nuclei from $^{278-320}120$ is given in the Figures 10 and 11, which also exhibits similar results. From our calculations, based on the Coulomb and Proximity Potential Model, we could find that the probability for the emission of 1n- and 2n- halo is considerably lower and significant probability is obtained only at the high mass end of superheavy elements. Similar results were obtained by K.P. Santhosh et al., for the emission of 1n- and 2n- halo nuclei from elements in the heavy region [50]. Also, many calculations showed that there exists much more probability for the emission of other cluster nuclei than the halo nuclei in an isotope family. For example, among the various isotopes of Florin, the decay of ^{23}F cluster from elements in super heavy region showed minimum value for the half-life of decay [37, 64]. Even though the probability for the emission of halo nuclei is less from superheavy elements, we have reported the emission of certain nuclei with decay half-life less than the upper experimental limit. We hope that, with the recent developments in experimental techniques, in near future, such emissions can be detected. Moreover, we hope that our studies will be helpful in the synthesis of new superheavy elements.

Further, the plot of $\log_{10} T_{1/2}$ versus the neutron number of parents gives an insight about neutron shell closure and the existence of neutron magic numbers. The nature of plot of half-life of decay versus the neutron number of parents or daughters can be used for predicting the neutron and proton magic numbers [65]. The neutron shell closure plays a crucial role in determining the stability of a nucleus against cluster decay. A peak in the plot represents the shell closure of parent nucleus and a dip in the plot represents the shell closure of daughter nuclei from the decay of parent corresponding to the dip. A closed neutron shell structure provides stability to the nucleus. Usually, neutron shell closure occurs at neutron magic numbers.

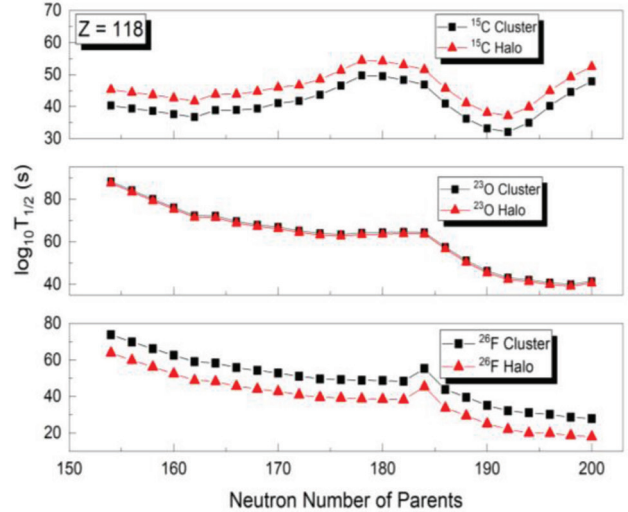


Figure 8: Comparison of the predicted heavy particle decay half-lives of cluster and the neutron halo, ^{15}C , ^{23}O and ^{26}F from $^{272-318}118$ even-even nuclei.

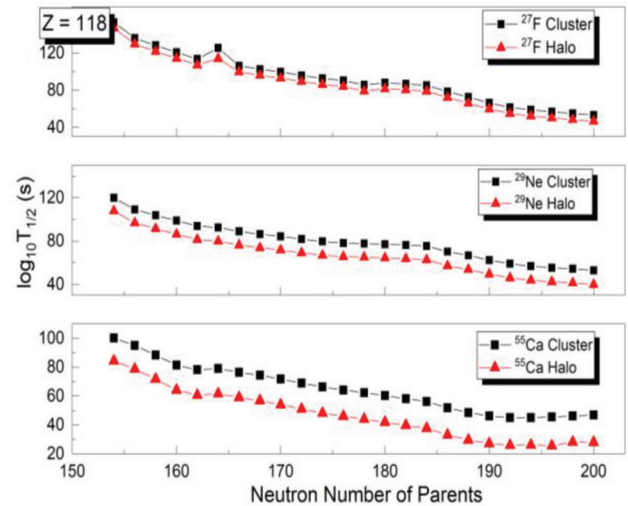


Figure 9: Comparison of the predicted heavy particle decay half-lives of cluster and the neutron halo, ^{27}F , ^{29}Ne and ^{55}Ca from $^{272-318}118$ even-even nuclei.

In Figure 6, there is a peak at $N_p = 150$ in all the three plots. Also, there is a peak at $N_p = 184$, in the plots of ^{23}O

and ^{26}F . In Figure 7, there is a peak at $N_p = 150$ in the plot of ^{29}Ne . This shows that the neutron shell closure of the parent occurs at neutron numbers 150 and 184. This indicates the stability of parent nuclei with $Z = 116$ against the decay of halo nuclei ^{15}C , ^{23}O , ^{26}F and ^{29}Ne at $N_p = 150$. Also, it is stable against the decay of ^{23}O and ^{26}F at $N_p = 184$. In Figure 7 and 8 there is a dip at $N_p = 162$, corresponding to the emission of ^{29}Ne from $^{264-316}116$ and ^{15}C from $^{272-318}118$ respectively, which indicates the stability of the daughter nuclei formed. In Figure 8, a peak at $N_p = 184$ can be observed in all the plots and it shows that the $Z = 118$ parent is stable against the decay of ^{15}C , ^{23}O and ^{26}F at $N_p = 184$.

In Figure 9, there is a peak at $N_p = 164$, which indicates the stability of $^{282}118$ against the decay of ^{27}F halo nucleus due to neutron shell closure of the parent nucleus. In Figures 6, 8 and 10, a dip is observed at $N_p = 192$ corresponding to the emission of ^{15}C halo nucleus and indicates the shell closure of the daughter nucleus formed.

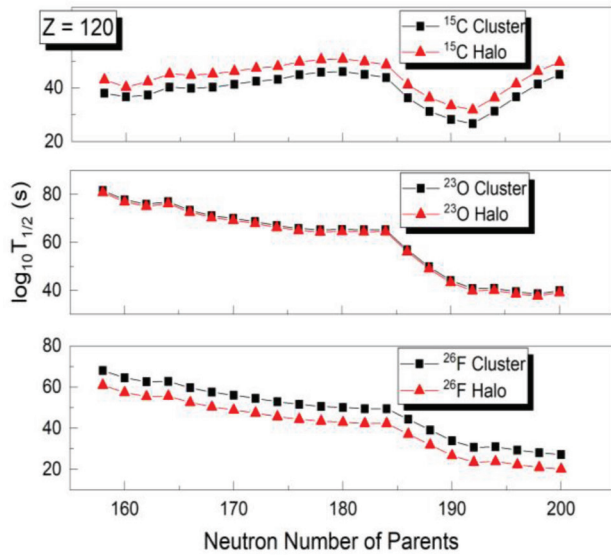


Figure 10: Comparison of the predicted heavy particle decay half-lives of cluster and the neutron halo, ^{15}C , ^{23}O and ^{26}F from $^{278-320}120$ even-even nuclei.

Thus, it is clear that the neutron shell closure occurs at 150, 164 and 184 and provides stability to the nucleus against the decay of halo nuclei. It is to be mentioned that 184 is already identified as a neutron magic number [65, 66, 67]. Usually it is observed that the predicted magic numbers vary with the method used to calculate the Q -value. In 2019, M. Ismail et al. [68], showed that the Q -values calculated from the finite-range droplet model predicted neutron magic numbers of 164, 170, 174, 180, 184 and 198, those based on the Weizsäcker-Skyrme model (WS4) indicated different neutron magic numbers of 172, 178, 184 and 196.

Both predicts only one magic number in common, i.e. 184. Ni et al. and Dong et al., also predicted the neutron shell closure at 164. [69, 70]. L. Satpathy and S.K. Patra predicted island of stability at neutron number 150 [71]. S. Cwiok et al. predicted neutron shell closure at 152 [72]. The nature of the plots of $\log_{10} T_{1/2}$ verses the neutron number of daughter nuclei, shows that neutron shell closure occurs at 164 and 184 which are already suggested as neutron magic numbers. The kink at $N_p = 150$, in Figure 6 and 7, suggests that neutron shell closure may occur at this neutron number.

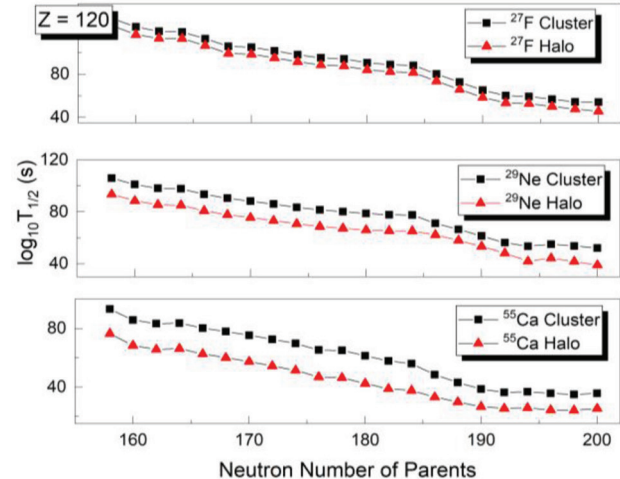


Figure 11: Comparison of the predicted heavy particle decay half-lives of cluster and the neutron halo, ^{27}F , ^{29}Ne and ^{55}Ca from $^{278-320}120$ even-even nuclei.

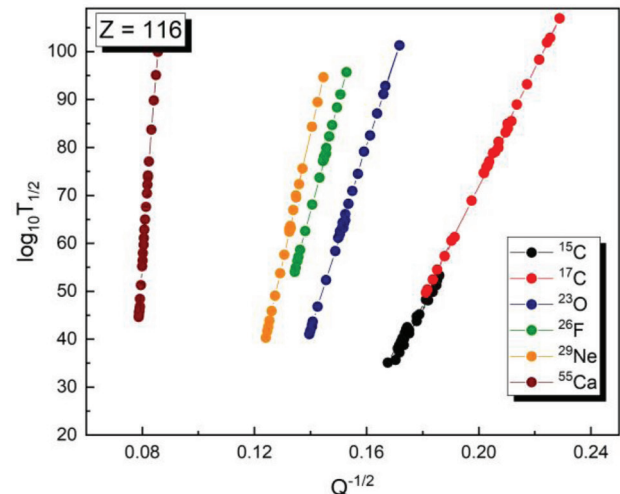


Figure 12: Geiger-Nuttall plot of $Q^{-1/2}$ versus $\log_{10} T_{1/2}$ for various neutron halo nuclei from super-heavy nuclei with $Z = 116$.

Figures 12-14 represents the plot of $Q^{-1/2}$ verses $\log_{10} T_{1/2}$ for the emission of halo nuclei from the isotopes of $Z = 116$, 118 and 120 elements. The plot is known as the Geiger-Nuttall

plot. The law was proposed by Geiger and Nuttall in 1911 to explain the alpha decay process. They found that the logarithmic value of half-life of decay varies linearly with the square root of the Q-value according to the expression [73];

$$\log_{10} T_{1/2} = MQ^{-1/2} + C \quad (16)$$

where M is the slope of the plot and C is the y-intercept. In 2012, Chong Qi et al. [74], showed that the Geiger Nuttall law can be successfully applied to cluster radioactivity also. From the linearity of the plots in the Figures 12-14, we can see that the Geiger Nuttall law can be applied to decay of halo nuclei also.

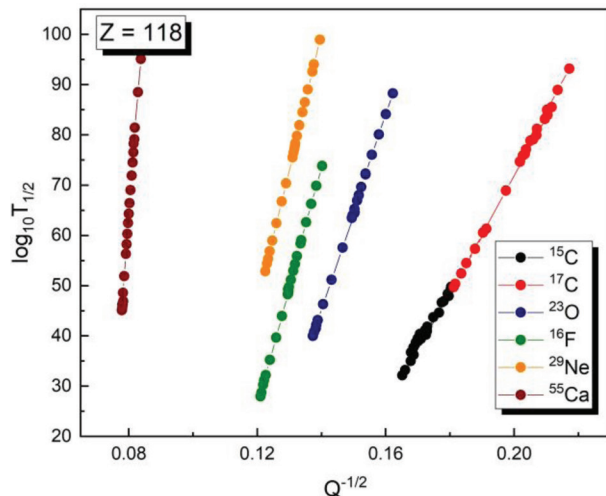


Figure 13: Geiger-Nuttall plot of $Q^{-1/2}$ verses $\log_{10} T_{1/2}$ for various neutron halo nuclei from super-heavy nuclei with $Z = 118$.

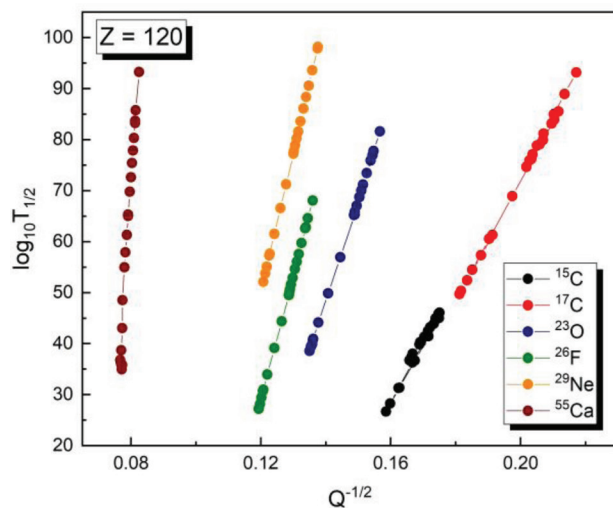


Figure 14: Geiger-Nuttall plot of $Q^{-1/2}$ verses $\log_{10} T_{1/2}$ for various neutron halo nuclei from super-heavy nuclei with $Z = 118$.

It is to be noted that Geiger-Nuttall law assumes only Coulomb interaction, in the model used in our calculations, the interaction potential is assumed as the sum of Coulomb, proximity and centrifugal potentials. However, we have neglected the centrifugal part by assuming zero momentum transfer. Therefore, it is clear that the linearity of the plot is not affected considerably by the inclusion of the proximity potential and the CPPM can explain the decay of halo nuclei from super heavy elements successfully.

Finally, Figure 15 shows the universal curve between $\log_{10} T_{1/2}$ and the negative logarithm of barrier penetrability ($-\ln P$) for the decay of ^{15}C , ^{23}O , ^{26}F and ^{55}Ca halo nuclei from $Z = 120$ parent isotopes. All the plots have the same slopes but different intercepts. The linearity of the universal curve confirms the validity of Geiger-Nuttall law in the case of emission of halo nuclei and also justifies the application of CPPM for describing the halo emission.

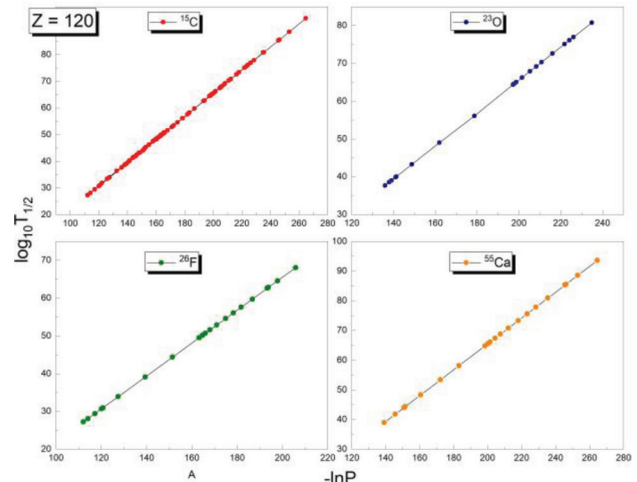


Figure 15: The universal curve for calculated logarithmic half-lives versus negative logarithm of penetrability for various neutron halos from the super-heavy nuclei with $Z = 120$.

Conclusion

The decay half-life of 1n and 2n halo nuclei from $^{270-316}116$, $^{272-318}118$ and $^{278-320}120$ is studied within the frame work of Coulomb and Proximity Potential Model. The halo structure is identified by calculating the 1n- and 2n- separation energies and by observing the cluster + core configuration corresponding to the minimum value of the driving potential. The decay half-life is compared by considering the neutron halo nuclei as a normal spherical cluster and as a halo with a rms radius. Our calculations show that the decay half-life for ^{26}F and ^{55}Ca nuclei is less than the experimental upper limit and no evidence for the emission of 2n halo nuclei is found in our results. Except

for ^{15}C , the emission probability is increased when the rms radius is considered. Also, the occurrence of neutron shell closure at neutron numbers 150, 164 and 184 became evident from the plot of $\log_{10} T_{1/2}$ versus the neutron number of parents. The linearity of the Geiger-Nuttall plots and the universal curve shows that Geiger-Nuttall law can be applied to halo nucleus also and it confirms the validity of CPPM for describing the decay of halo nuclei from super-heavy elements. We strongly believe that our study will help the researchers for proceeding further towards the structure and properties of halo nuclei and proceeding towards the synthesis of new super-heavy elements.

References

- [1] L. Neufcourt, Y. Cao, W. Nazarewicz, E. Olsen and F. Viens, Phys. Rev. Lett. **122**, 062502 (2019). <https://doi.org/10.1103/physrevlett.122.062502>
- [2] J. Al-Khalili, F. Nunes, J. Phys. G: Nucl. Part. Phys. **29**, R89 (2003). <https://doi.org/10.1088/0954-3899/29/11/r01>
- [3] P.G. Hansen, A.S. Jensen and B. Jonson, Nuclear halos. Annu. Rev. Nucl. Part. Sci. **45**, 591 (1995). <https://doi.org/10.1146/annurev.ns.45.120195.003111>
- [4] I. Tanihata, H. Hamagaki, O. Hashimoto, Y. Shida, N. Yoshikawa, K. Sugimoto, O. Yamakawa, T. Kobayashi and N. Takahashi, Phys. Rev. Lett. **55**, 2676 (1985). <https://doi.org/10.1103/physrevlett.55.2676>
- [5] P.G. Hansen and B. Jonson, Euro. Phys. News **4**, 409 (1987). <https://doi.org/10.1209/0295-5075/4/4/005>
- [6] I. Tanihata, H. Hamagaki, O. Hashimoto, S. Nagamiya, Y. Shida, N. Yoshikawa, O. Yamakawa, K. Sugimoto, T. Kobayashi, D.E. Greiner, N. Takahashi and Y. Nojiri, Phys. Lett. B **160**, 380 (1985). [https://doi.org/10.1016/0370-2693\(85\)90005-X](https://doi.org/10.1016/0370-2693(85)90005-X)
- [7] J. Al-Khalili, Lect. Notes Phys. **651**, 77 (2004). https://doi.org/10.1007/978-3-540-44490-9_3
- [8] T. Suzuki, T. Otsuka, C. Yuan and N. Alahari, Phys. Lett. B **753**, 199 (2016). <https://doi.org/10.1016/j.physletb.2015.12.001>
- [9] L. Gaudefroy, W. Mittig, N.A. Orr, S. Varet, M. Chartier, P. Roussel-Chomaz, J.P. Ebran, B. Fernandez-Dominguez, G. Fremont, P. Gangnaut, A. Gillibert, S. Grevy, J.F. Libin, V.A. Maslov, S. Paschal, B. Pietras, Yu.-E. Penionzhkevich, C. Spitaels and A.C.C. Villari, Phys. Lett. B, **109**, 202503 (2012). <https://doi.org/10.1103/PhysRevLett.109.202503>
- [10] S.G. Zhou, J. Meng, P. Ring and E.-G. Zhao, Phys. Rev. C **82**, 011301 (2010). <https://doi.org/10.1103/physrevc.82.011301>
- [11] T. Nakamura, N. Kobayashi, Y. Kondo, Y. Satou, N. Aoi, H. Baba, S. Deguchi, N. Fukuda, J. Gibelin, N. Inabe, M. Ishihara, D. Kameda, Y. Kawada, T. Kubo, K. Kusaka, A. Mengoni, T. Motobayashi, T. Ohnishi, M. Ohtake, N.A. Orr, H. Otsu, T. Otsuka, A. Saito, H. Sakurai, S. Shimoura, T. Sumikama, H. Takeda, E. Takeshita, M. Takechi, S. Takeuchi, K. Tanaka, K. N. Tanaka, N. Tanaka, Y. Togano, Y. Utsuno, K. Yoneda, A. Yoshida, and K. Yoshida, Phys. Rev. Lett. **103**, 262501 (2009). <https://doi.org/10.1103/physrevlett.103.262501>
- [12] D. Bazin, B.A. Brown, J. Brown, M. Fauerbach, M. Hellstrom, S.E. Hirzebruch, J.H. Kelley, R.A. Kryger, D.J. Morrissey, R. Pfaff, C.F. Powell, B.M. Sherrill and M. Thoennessen, Phys. Rev. Lett. **74**, 3569 (1995). <https://doi.org/10.1103/physrevlett.74.3569>
- [13] R. Bhattacharya and K. Krishan, Phys. Rev. C **56**, 212 (1997). <https://doi.org/10.1103/physrevc.56.212>
- [14] K. Varga, R.G. Lovas and R.J. Liotta, Phys. Rev. Lett. **69**, 37 (1992). <https://doi.org/10.1103/physrevlett.69.37>
- [15] M. Patial, R.J. Liotta, R. Wyss, Phys. Rev. C, **93**, 054326 (2016) <https://doi.org/10.1103/physrevc.93.054326>
- [16] C. Xu, G. Röpke, P. Schuck, Z. Ren, Y. Funaki, H. Horiuchi and B. Zhou, Phys. Rev. C **95**, 061306 (2017). <https://doi.org/10.1103/physrevc.95.061306>
- [17] Y.K. Gambhir, P. Ring and A. Thimet, Ann. Phys. **198**, 132 (1990). [https://doi.org/10.1016/0003-4916\(90\)90330-q](https://doi.org/10.1016/0003-4916(90)90330-q)
- [18] M.V. Zhukov, B.V. Danilin, D.V. Fedorov, J.M. Bang, I.J. Thompson and J.S. Vaagen, Phys. Rep. **231**, 151 (1993). [https://doi.org/10.1016/0370-1573\(93\)90141-y](https://doi.org/10.1016/0370-1573(93)90141-y)
- [19] S.-G. Zhou, J. Meng, P. Ring and E.-G. Zhao, Phys. Rev. C **82**, 011301(R) (2010). <https://doi.org/10.1103/physrevc.82.011301>
- [20] B.V. Danilin, S.N. Ershov and J.S. Vaagen, Phys. Rev. C **71**, 057301 (2005). <https://doi.org/10.1103/PhysRevC.71.057301>
- [21] F. Robicheaux, Phys. Rev. A **60**, 1706 (1999). <https://doi.org/10.1103/physreva.60.1706>
- [22] M.T. Yamashita, Lauro Tomio and T. Fredericoc, Nucl. Phys. A **735**, 40 (2004). <https://doi.org/10.1016/j.nuclphysa.2004.02.003>
- [23] M. Takechi, S. Suzuki, D. Nishimura, M. Fukuda, T. Ohtsubo, M. Nagashima, T. Suzuki, T. Yamaguchi, A. Ozawa, T. Moriguchi, H. Ohishi, T. Sumikama, H. Geissel, N. Aoi, R.J. Chen, D.Q. Fang, N. Fukuda, S. Fukuoka, H. Furuki, N. Inabe, Y. Ishibashi, T.

- Itoh, T. Izumikawa, D. Kameda, T. Kubo, M. Lantz, C.S. Lee, Y.G. Ma, K. Matsuta, M. Mihara, S. Momota, D. Nagae, R. Nishikiori, T. Niwa, T. Ohnishi, K. Okumura, M. Ohtake, T. Ogura, H. Sakurai, K. Sato, Y. Shimbara, H. Suzuki, H. Takeda, S. Takeuchi, K. Tanaka, M. Tanaka, H. Uenishi, M. Winkler, Y. Yanagisawa, S. Watanabe, K. Minomo, S. Tagami, M. Shimada, M. Kimura, T. Matsumoto, Y.R. Shizmizu and M. Yahiro, Phys. Rev. C **90**, 061305 (2014). <https://doi.org/10.1103/physrevc.90.061305>
- [24] N. Kobayashi, T. Nakamura, Y. Kondo, J.A. Tostevin, Y. Utsuno, N. Aoi, H. Baba, R. Barthelemy, M.A. Faminiano, N. Fukuda, N. Inabe, M. Ishihara, R. Kanungo, S. Kim, T. Kubo, G.S. Lee, H.S. Lee, M. Matsushita, T. Motobayashi, T. Ohnishi, N.A. Orr, H. Otsu, T. Otsuka, T. Sako, H. Sakurai, Y. Satou, T. Sumikama, H. Takeda, S. Takeuchi, R. Tanaka, Y. Togano and K. Yoneda, Phys. Rev. Lett. **112**, 242501 (2014). <https://doi.org/10.1103/physrevlett.112.242501>
- [25] I. Tanihata, J. Phys. G: Nucl. Part. Phys. **22**, 157 (1996). <https://doi.org/10.1088/0954-3899/22/2/004>
- [26] R. Kumari, Nucl. Phys. A **917**, 85 (2013). <https://doi.org/10.1016/j.nuclphysa.2013.09.001>
- [27] E.F. Aguilera, P.A. Valenzuela, E.M. Quiroz, J.F. Arnaiz, J.J. Kolata and V. Guimaraes, Phys. Rev. C **93**, 034613 (2016). <https://doi.org/10.1103/physrevc.93.034613>
- [28] J.A. Tostevin, F.M. Nunes and I.J. Thompson, Phys. Rev. C **63**, 024617 (2001). <https://doi.org/10.1103/physrevc.63.024617>
- [29] V. Rotival and T. Duguet, Phys. Rev. C **79**, 054308 (2009). <https://doi.org/10.1103/physrevc.79.054308>
- [30] A. Calci, P. Navrátil, R. Roth, J. Dohet-Eraly, S. Quaglioni and G. Hupin, Phys. Rev. Lett., **117**, 242501 (2016). <https://doi.org/10.1103/physrevlett.117.242501>
- [31] M. Takechi, T. Ohtsubo, M. Fukuda, D. Nishimura, T. Kuboki, T. Suzuki, T. Yamaguchi, A. Ozawa, T. Moriguchi, H. Ooishi, D. Nagae, H. Suzuki, S. Suzuki, T. Izumikawa, T. Sumikama, M. Ishihara, H. Geissel, N. Aoi, Rui-Jiu Chen, De-Qing Fang, N. Fukuda, I. Hachiuma, N. Inabe, Y. Ishibashi, Y. Ito, D. Kameda, T. Kubo, K. Kusaka, M. Lantz, Yu-Gang Ma, K. Matsuta, M. Mihara, Y. Miyashita, S. Momota, K. Namihira, M. Nagashima, Y. Ohkuma, T. Ohnishi, M. Ohtake, K. Ogawa, H. Sakurai, Y. Shimbara, T. Suda, H. Takeda, S. Takeuchi, K. Tanaka, R. Watanabe, M. Winkler, Y. Yanagisawa, Y. Yasuda, K. Yoshinaga, A. Yoshida and K. Yoshida, Phys. Lett. B **707**, 357 (2012). <https://doi.org/10.1016/j.physletb.2011.12.028>
- [32] K.P. Aanjali, K. Prathapan and R.K. Biju, Braz. J. Phys. **50**, 71 (2019) <https://doi.org/10.1007/s13538-019-00719-9>
- [33] K.P. Aanjali, K. Prathapan and R.K. Biju, Nucl. Phys. A **993**, 121644 (2020) <https://doi.org/10.1016/j.nuclphysa.2019.121644>
- [34] K.P. Santhosh, R.K. Biju and A. Joseph, J. Phys. G: Nucl. Part. Phys. **35**, 085102 (2008). <https://doi.org/10.1088/0954-3899/35/8/085102>
- [35] K.P. Santhosh and R.K. Biju, J. Phys. G: Nucl. Part. Phys. **36**, 015107 (2009). <https://doi.org/10.1088/0954-3899/36/1/015107>
- [36] K.P. Santhosh and C. Nithya, At. Dat. and Nucl. Dat. Tabls. **119**, 33 (2018). <https://doi.org/10.1016/j.adt.2017.03.003>
- [37] K. Prathapan, K.P. Anjali and R.K. Biju, Braz. J. Phys. **49** 752 (2019). <https://doi.org/10.1007/s13538-019-00681-6>
- [38] Y.J. Shi and W.J. Swiatecki, Nucl. Phys. A **438**, 450 (1985). [https://doi.org/10.1016/0375-9474\(85\)90385-9](https://doi.org/10.1016/0375-9474(85)90385-9)
- [39] J. Blocki, J. Randrup, W.J. Swiatecki and C.F. Tsang, Ann. Phys. **105**, 427 (1977). [https://doi.org/10.1016/0003-4916\(77\)90249-4](https://doi.org/10.1016/0003-4916(77)90249-4)
- [40] J. Blocki and W.J. Swiatecki, Ann. Phys. **132**, 53 (1981). [https://doi.org/10.1016/0003-4916\(81\)90268-2](https://doi.org/10.1016/0003-4916(81)90268-2)
- [41] K.P. Santhosh and B. Priyanka, Eur. Phys. J. A **49**, 66 (2013). <https://doi.org/10.1140/epja/i2013-13066-y>
- [42] D.N. Poenaru, M. Ivascu, A. Sandulescu and W. Greiner, Phys. Rev. C **32**, 572 (1985). <https://doi.org/10.1103/physrevc.32.572>
- [43] S. S. Malik and R.K. Gupta, Phys. Rev. C **39**, 1992 (1989). <https://doi.org/10.1103/physrevc.39.1992>
- [44] K.P. Santhosh, Sabina Sahadevan and R.K. Biju, Nucl. Phys. A **825**, 159 (2009). <https://doi.org/10.1016/j.nuclphysa.2009.04.01>
- [45] K.P. Santhosh, J.G. Joseph and S. Sahadevan, Phys. Rev. C **82**, 064605 (2010). <https://doi.org/10.1103/physrevc.82.064605>
- [46] K.P. Santhosh and B. Priyanka, Phys. Rev. C **87**, 064611 (2013). <https://doi.org/10.1103/physrevc.87.064611>
- [47] K. P. Santhosh, B. Priyanka, J.G. Joseph and S. Sahadevan, Phys. Rev. C **84**, 024609 (2011). <https://doi.org/10.1103/physrevc.84.024609>
- [48] K. P. Santhosh and Indu Sukumaran, Phys. Rev. C **96**, 034619 (2017). <https://doi.org/10.1103/physrevc.96.034619>

- [49] K.P. Santhosh and I. Sukumaran, *Pramana.*, **J. Phys.** **92**, 6 (2019). <https://doi.org/10.1007/s12043-018-1672-4>
- [50] K.P. Santhosh and I. Sukumaran, *Braz J. Phys.* **48**, 497 (2018). <https://doi.org/10.1007/s13538-018-0585-5>
- [51] R.K. Gupta, S. Kumar, M. Balasubramaniam, G. Munzenberg and W. Scheid, *J. Phys. G: Nucl. Part. Phys.* **28**, 699 (2002). <https://doi.org/10.1088/0954-3899/28/4/309>
- [52] M. Wang, G. Audi, F.G. Kondev, W.J. Huang, S. Naimi and X. Xu, *Chin. Phys. C* **41**, 030003 (2017). <https://doi.org/10.1088/1674-1137/41/3/030003>
- [53] A. Leistenschneider, T. Aumann, K. Boretzky, D. Cortina, J. Cub, U.D. Pramanik, W. Dostal, T.W. Elze, H. Emling, H. Geissel, A. Grünschlob, M. Hellstr, R. Holzmann, S. Ilievski, N. Iwasa, M. Kaspar, A. Kleinböhl, J.V. Kratz, R. Kulessa, Y. Leifels, E. Lubkiewicz, G. Münzenberg, P. Reiter, M. Rejmund, C. Scheidenberger, C. Schlegel, H. Simon, J. Stroth, K. Sümerer, E. Wajda, W. Walús and S. Wan, *Phys. Rev. Lett.* **86**, 5442 (2001). <https://doi.org/10.1103/physrevlett.86.5442>
- [54] H. Simon, D. Aleksandrov, T. Aumann, L. Axelsson, T. Baumann, M.J.G. Borge, L.V. Chulkov, R. Collatz, J. Cub, W. Dostal, B. Eberlein, T.W. Elze, H. Emling, H. Geissel, A. Grünschloss, M. Hellström, J. Holeczek, R. Holzmann, B. Jonson, J.V. Kratz, G. Kraus, R. Kulessa, Y. Leifels, A. Leistenschneider, T. Leth, I. Mukha, G. Münzenberg, F. Nickel, T. Nilsson, G. Nyman, B. Petersen, M. Pfützner, A. Richter, K. Riisager, C. Scheidenberger, G. Schrieder, W. Schwab, M.H. Smedberg, J. Stroth, A. Surowiec, O. Tengblad, M.V. Zhukov, *Phys. Rev. Lett.* **83**, 496 (1999). <https://doi.org/10.1103/physrevlett.83.496>
- [55] T. Nakamura, N. Kobayashi, Y. Kondo, Y. Satou, J. A. Tostevin, Y. Utsuno, N. Aoi, H. Baba, N. Fukuda, J. Gibelin, N. Inabe, M. Ishihara, D. Kameda, T. Kubo, T. Motobayashi, T. Ohnishi, N. A. Orr, H. Otsu, T. Otsuka, H. Sakurai, T. Sumikama, H. Takeda, E. Takeshita, M. Takechi, S. Takeuchi, Y. Togano and K. Yoneda, *Phys. Rev. Lett.* **112**, 242501 (2014). <https://doi.org/10.1103/physrevlett.112.142501>
- [56] Manju, J. Singh, Shubhchintak and R. Chatterjee, *Eur. Phys. J. A* **55**, 5 (2019). <https://doi.org/10.1140/epja/i2019-12679-4>
- [57] Z. Ren, B. Chen, Z. Ma, Z. Zhu and G. Xu, *J. Phys. G: Nucl. Part. Phys.* **22**, 523 (1996). <https://doi.org/10.1088/0954-3899/22/4/013>
- [58] H. Koura, *Progress in Theoretical Physics* **113**, 305 (2005). <https://doi.org/10.1143/ptp.113.305>
- [59] V.Y. Denisov and H. Ikezoe, *Phys. Rev. C* **72**, 064613 (2005). <https://doi.org/10.1103/physrevc.72.064613>
- [60] K.N. Huang, M. Aoyagi, M.H. Chen, B. Crasemann and H. Mark, *At. Data Nucl. Data Tables* **18**, 243 (1976). [https://doi.org/10.1016/0092-640x\(76\)90027-9](https://doi.org/10.1016/0092-640x(76)90027-9)
- [61] A. Ozawa, T. Suzuki and I. Tanihata, *Nucl. Phys. A* **693**, 32 (2001). [https://doi.org/10.1016/S0375-9474\(01\)01152-6](https://doi.org/10.1016/S0375-9474(01)01152-6)
- [62] P. Moller, A. J. Sierk, T. Ichikawa and H. Sagawa, *Atomic Data and Nuclear Data Tables* **109-110**, 1 (2016). <https://doi.org/10.1016/j.adt.2015.10.002>
- [63] Suhel Ahmad, A.A. Usmani and Z. A. Khan, *Phys. Rev. C* **96**, 064602 (2017). <https://doi.org/10.1103/physrevc.96.064602>
- [64] K.P. Santhosh and I. Sukumaran, *Int. J. Mod. Phys. E* **26**, 1750003 (2017). <https://doi.org/10.1142/s0218301317500033>
- [65] M. Ismail, W.M. Seif, A. Abdurrahman, *Phys. Rev. C* **94**, 024316 (2016). <https://doi.org/10.1103/physrevc.94.024316>
- [66] M. Ismail, A.Y. Ellithi, M.M. Botros and A. Adel, *Phys. Rev. C* **81**, 024602 (2010). <https://doi.org/10.1103/physrevc.81.024602>
- [67] R. K. Gupta, S.K. Patra and W. Greiner, *Mod. Phys. Lett. A* **12**, 1727 (1997). <https://doi.org/10.1142/s021773239700176x>
- [68] M. Ismail, W.M. Seif, W.M. Tawfik and A.M. Hussein, *Ann. Phys.* **406**, 1 (2019). <https://doi.org/10.1016/j.aop.2019.03.020>
- [69] D. Ni and Z. Ren, *Nucl. Phys. A* **893**, 13 (2012). <https://doi.org/10.1016/j.nuclphysa.2012.08.006>
- [70] T. Dong and Z. Ren, *Phys. Rev. C.*, **82**, 034320 (2010). <https://doi.org/10.1103/physrevc.82.034320>
- [71] L. Satpathy and S.K. Patra, *Nucl. Phys. A* **722**, 24c (2003). [https://doi.org/10.1016/s0375-9474\(03\)01330-7](https://doi.org/10.1016/s0375-9474(03)01330-7)
- [72] S. Cwiok, S. Hofmann and W. Nazarewicz, *Nucl. Phys. A* **573**, 356 (1994). [https://doi.org/10.1016/0375-9474\(94\)90349-2](https://doi.org/10.1016/0375-9474(94)90349-2)
- [73] H. Geiger and J.M. Nuttall, *Philos. Mag.* **22**, 613 (1911). <https://doi.org/10.1080/14786441008637156>
- [74] C. Qi, R.J. Liotta and R. Wyss, *J. Phys. Conf. Ser.* **381**, 012131 (2012). <https://doi.org/10.1088/1742-6596/381/1/012131>



Journal of Nuclear Physics, Material Sciences, Radiation and Applications

Chitkara University, Saraswati Kendra, SCO 160-161, Sector 9-C,
Chandigarh, 160009, India

Volume 8, Issue 1

August 2020

ISSN 2321-8649

Copyright: [© 2020 K. Prathapan, K.P. Anjali and R.K. Biju] This is an Open Access article published in Journal of Nuclear Physics, Material Sciences, Radiation and Applications (J. Nucl. Phy. Mat. Sci. Rad. A.) by Chitkara University Publications. It is published with a Creative Commons Attribution- CC-BY 4.0 International License. This license permits unrestricted use, distribution, and reproduction in any medium, provided the original author and source are credited.
